Origin of the nonlinear second-order optical susceptibilities of organic systems

Salvatore J. Lalama and Anthony F. Garito
Department of Physics and Laboratory for Research on the Structure of Matter, University of Pennsylvania, Philadelphia, Pennsylvania 19104
(Received 9 May 1979)

An all-valence-electron self-consistent-field linear-combination-of-atomic-orbitals molecular-orbital procedure including configuration interactions for calculating the magnitude and sign of the nonlinear second-order molecular susceptibility components (hyperpolarizability) for substituted dipolar aromatic molecular systems is reported. Three fundamentally important examples, aniline, nitrobenzene, and *p*-nitroaniline, are considered. Analysis of the microscopic origin of their molecular second-order susceptibilities provides a direct means for understanding the macroscopic nonlinear optical response of organic molecular solids which have already been observed to possess exceptional nonlinear optical properties. The important excited states of aniline, nitrobenzene, and *p*-nitroaniline have been identified and examined in their relationship with the molecular second-order susceptibility-tensor components β_{ijk}. The detailed nature of the charge separation accompanying these states has been discussed in terms of both the configurations composing the excited states, and also the one-electron molecular orbitals which determine those configurations. These results demonstrate how the bond-additivity approximation is inappropriate for *p*-nitroaniline. Finally, the frequency dependence of the β_{ijk} components in each case shows that the Kleinman relations are valid approximations only at relatively low frequencies.

I. INTRODUCTION

Recently considerable interest has centered around the unusually large nonlinear second-order optical susceptibilities of organic solids and liquids.[1-33] Commonly these solids and liquids are composed of dipolar aromatic molecules that are substituted with π-electron donors and acceptors and exhibit intramolecular charge transfer between the two groups.[34,35] As discussed by Davydov and co-workers, Levine and Bethea, and Oudar, Chemla, and co-workers, the resulting charge transfer states are believed to play a dominant role in contributions to the observed optical nonlinearities. Present descriptions such as phenomenological two-level models[14,23,36] appear inadequate to account for these contributions, and questions concerning the validity of bond additivity and the dispersion of nonlinear susceptibilities remain. It would thus be desirable to obtain a suitable microscopic description that relates the properties of the charge-separated states with the nonlinear second-order optical susceptibilities.

In this paper, we report an all-valence-electron self-consistent-field linear-combination-of-atomic-orbitals molecular-orbital (SCFLCAO MO) procedure including configuration interactions for calculating the magnitude and sign of the nonlinear second-order molecular susceptibility components (hyperpolarizability) for substituted dipolar aromatic molecules. Since our principal interest is organic solids and polymers, the understanding of microscopic second-order molecular susceptibilities β_{ijk} is motivated by the fact that the crystal macroscopic second-order susceptibility $\chi^{2\omega}_{ijk}(-2\omega;\omega,\omega)$ can be expressed as a sum of N molecular contributions

$$\chi^{2\omega}_{ijk}(-2\omega;\omega,\omega)=Nf_{ii}f_{jj}f_{kk}\beta_{ijk}(-2\omega;\omega,\omega)\,, \quad (1)$$

where β_{ijk} is determined from vapor-phase or liquid-solution measurements and terms such as f_{ii} represent local-field corrections. Three fundamentally important examples, aniline, nitrobenzene, and *p*-nitroaniline, are considered. Crystals of nitroaniline derivatives exhibit the largest nonlinear second-order susceptibilities reported to date for organic solids.[1,7,19,28,29,37] Aniline and nitrobenzene provide relevant limiting cases where the benzene ring is substituted separately in each case with an electron donor (NH_2) and an acceptor (NO_2) group. Their study is intended to define how the interaction between the benzene ring and the different substituent groups manifests itself in the tensor components of β_{ijk}.

Aniline, nitrobenzene, and *p*-nitroaniline, molecular structures of which are given in Fig. 1, belong to the C_{2v} point group. The coordinate origins are chosen as centered in the molecular rings with the x axis along the permanent dipole moment direction and the z axis normal to the molecular plane. The nonzero tensor components of β_{ijk} are β_{xxx}, β_{xyy}, β_{xzz}, β_{yxy}, β_{yyx}, β_{zxz}, and β_{zzx}, where for second-harmonic generation $\beta_{yyx}=\beta_{yxy}$ and $\beta_{zzx}=\beta_{zxz}$. When the Kleinman relations[38] apply, the distinct nonzero components reduce to just β_{xxx}, β_{xyy}, and β_{xzz}. In Sec. II we present a theoretical description for calculating the tensor components of β_{ijk} based on SCFLCAO MO[39]

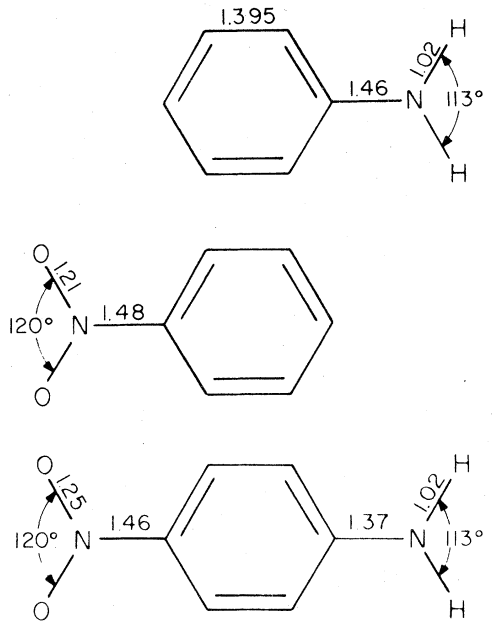

FIG. 1. Molecular structures of aniline, nitrobenzene, and p-nitroaniline.

methods including configuration interactions.[40,41] In Sec. III a semiempirical parametrization method using the computationally accessible CNDO method is outlined. Comparisons are made between the calculated electron structures and experimental photoemission and ultraviolet absorption data for each case. In Sec. IV the calculations of the tensor components of β_{ijk} are presented for aniline, nitrobenzene, and p-nitroaniline. The calculated results are examined in detail to trace the important contributions to β_{ijk} in each system. The question of bond additivity is addressed, and the frequency dependence of the β_{ijk} components is presented to see where the Kleinman symmetry relations remain valid.

II. DESCRIPTION OF MOLECULAR SECOND-ORDER SUSCEPTIBILITY

In the frequency range above vibrational and rotational modes and below electronic resonances, the dipole approximation with the perturbing Hamiltonian $H' = \vec{E}^{\omega} \cdot \vec{r} \sin\omega t$ yields the electronic second-order susceptibility β_{ijk} expressed in the following convenient form[42]:

$$\beta_{ijk}+\beta_{ikj}=-\frac{e^3}{4\hbar^2}\Bigg[\sum_{\substack{n\neq n'\\ n\neq g\\ n'\neq g}}(r^j_{gn'}r^i_{n'n}r^k_{gn}+r^k_{gn'}r^i_{n'n}r^j_{gn})\left(\frac{1}{(\omega_{n'g}-\omega)(\omega_{ng}+\omega)}+\frac{1}{(\omega_{n'g}+\omega)(\omega_{ng}-\omega)}\right)$$
$$+(r^i_{gn'}r^j_{n'n}r^k_{gn}+r^i_{gn'}r^k_{n'n}r^j_{gn})\left(\frac{1}{(\omega_{n'g}+2\omega)(\omega_{ng}+\omega)}+\frac{1}{(\omega_{n'g}-2\omega)(\omega_{ng}-\omega)}\right)$$
$$+(r^j_{gn'}r^k_{n'n}r^i_{gn}+r^k_{gn'}r^j_{n'n}r^i_{gn})\left(\frac{1}{(\omega_{n'g}-\omega)(\omega_{ng}-2\omega)}+\frac{1}{(\omega_{n'g}+\omega)(\omega_{ng}+2\omega)}\right)$$
$$+4\sum_{n}\left[r^j_{gn}r^k_{gn}\Delta r^i_n(\omega^2_{ng}-4\omega^2)+r^i_{gn}(r^k_{gn}\Delta r^j_n+r^j_{gn}\Delta r^k_n)(\omega^2_{ng}+2\omega^2)\right]\frac{1}{(\omega^2_{ng}-\omega^2)(\omega^2_{ng}-4\omega^2)}\Bigg], \tag{2}$$

where summations are over complete sets of eigenstates Ψ_n and $\Psi_{n'}$ of the unperturbed molecular system. The quantities such as r^i_{gn} and $r^i_{nn'}$ are matrix elements of the ith components of the dipole operator for the molecule between the unperturbed ground and excited states and between two excited states, respectively; $\Delta r^i_n \equiv r^i_{nn} - r^i_{gg}$ is the difference between the excited- and ground-state dipole moments, ω the frequency of the applied electric field, and ω_{ng} the difference between excited- and ground-state energies.

The second-order susceptibility expression [Eq. (2)] can be evaluated by means of molecular Hartree-Fock theory as given by Roothaan.[39,43] In this formalism the unperturbed ground-state wave function Ψ_g for a closed-shell system of $2l$ electrons is expressed as a single antisymmetrized product of molecular-orbital functions ψ_i:

$$\Psi_g = \det\left|\psi_1\bar{\psi}_1\cdots\psi_i\bar{\psi}_i\cdots\psi_l\bar{\psi}_l\right| . \tag{3}$$

The elements of the determinantal wave functions are represented in the LCAO approximation as

$$\psi_i = \sum_{\mu} c_{\mu i}\phi_{\mu} , \tag{4}$$

where ϕ_{μ} are atomic orbitals. The coefficients of the atomic orbitals are calculated self-consistently through Roothaan's equations to obtain the ψ_i and the corresponding one-electron energies ϵ_i:

$$\sum_{\nu}(F_{\mu\nu}-\epsilon_i S_{\mu\nu})c_{\nu i}=0 , \tag{5}$$

where the Fock matrix $F_{\mu\nu}$ and overlap integrals

$S_{\mu\nu}$ are given by

$$F_{\mu\nu}=H_{\mu\nu}+\sum_{\lambda\sigma}P_{\lambda\sigma}[(\mu\nu|\lambda\sigma)-\tfrac{1}{2}(\mu\lambda|\nu\sigma)] \quad (6a)$$

and

$$S_{\mu\nu}=\int\phi_\mu\phi_\nu d\tau\,. \quad (6b)$$

Here the core Hamiltonian matrix $H_{\mu\nu}$, density matrix $P_{\mu\nu}$, and two-electron repulsion integrals are given by

$$H_{\mu\nu}=\int\phi_\mu H^{\text{core}}\phi_\nu d\tau\,, \quad (6c)$$

$$P_{\mu\nu}=2\sum_{i=1}^{\text{occupied}}c_{\mu i}c_{\nu i}\,, \quad (6d)$$

and

$$(\mu\nu|\lambda\sigma)=\int\phi_\mu(1)\phi_\nu(1)\frac{1}{r_{12}}\phi_\lambda(2)\phi_\sigma(2)d\tau_1\,d\tau_2\,, \quad (6e)$$

and the molecular Hamiltonian by

$$H=\sum_i H_i^{\text{core}}+\sum_{i<j}\frac{1}{r_{ij}}\,,\quad H_i^{\text{core}}=-\tfrac{1}{2}\nabla_i^2-\sum_A\frac{Z_A}{r_{Ai}}\,, \quad (6f)$$

where the sum on $i(A)$ is over electrons (nucleii), and Z_A is the net core charge.

The excited-state wave functions Ψ_n are expressed as a linear combination of configuration functions restricted to singly-excited configurations

$$\Psi_n=\sum_{i,j}A_{n,i\to j}\chi_{i\to j}\,, \quad (7)$$

with $\chi_{i\to j}$ an antisymmetrized product of one-electron molecular orbitals where because of symmetry, only spin singlet states need be considered. The wave functions and energy eigenvalues E_n of the excited states are determined by solving for $A_{n,i\to j}$ in the secular equation

$$\sum_{i,j,k,l}A_{n,i\to j}A_{n,k\to l}\langle\chi_{i\to j}|H-E_n|\chi_{k\to l}\rangle=0\,. \quad (8)$$

The dipole moment matrix elements $r^i_{nn'}$, r^i_{gn}, and Δr^i_n are expressed as sums of one-electron integrals[40]

$$r^i_{nn'}=\sum_{i,j,k,l}{}'A_{n,i\to j}A_{n',k\to l}\int\chi_{i\to j}M^i\chi_{k\to l}d\tau$$

$$=\sum_{i,j,k,l}{}'A_{n,i\to j}A_{n',k\to l}(\delta_{ik}m^i_{jl}-\delta_{jl}m^i_{ik})\,, \quad (9a)$$

$$r^i_{gn}=\sqrt{2}\sum_{i,j}A_{n,i\to j}m^i_{ij}\,, \quad (9b)$$

and

$$\Delta r^i_n=\sum_{i,j,k,l}{}'A_{n,i\to j}A_{n,k\to l}(\delta_{ik}m^i_{jl}-\delta_{jl}m^i_{ik})$$

$$+\sum_{i,j}|A_{n,i\to j}|^2(m^i_{jj}-m^i_{ii})\,. \quad (9c)$$

The primed summations are understood to exclude terms in which $i=k$ and $j=l$ simultaneously. M^i is the ith component of the molecular dipole operator

$$M^i=-\sum_\alpha r^i_\alpha+\sum_A Z_A R^i_A\,, \quad (10)$$

where r^i_α is the ith component of the position coordinate of the αth electron, and R^i_A is the ith component of the position of the Ath nucleus having net core charge Z_Ae. The m^i_{ij} are one-electron dipole integrals over molecular orbitals,

$$m^i_{ij}=\int\psi_i(\vec{r})r^i\psi_j(\vec{r})d\vec{r}$$

$$=\sum_{\mu\nu}c_{\mu i}c_{\nu j}\int\phi_\mu r^i\phi_\nu d\vec{r}\,, \quad (11)$$

where the integrals over atomic orbitals can be evaluated explicitly.

III. SEMIEMPIRICAL CALCULATION PROCEDURE

Our procedure in evaluating the expression for β_{ijk} [Eq. (2)] consists initially of a semiempirical parametrization method that is guided by two standard requirements: the one-electron eigenvalue solutions (ϵ_i) of the Roothaan equations [Eq. (5)] are to provide a suitable description of experimental photoemission data, and the configuration-interaction calculations of excited-state energies (E_n) and ground-to-excited-state transition moments (r^i_{gn}) are required to agree with ultraviolet absorption data. Finally, the calculated excited-state energies and ground-to-excited-state transition moments are used along with the dipole moment matrix elements $r^i_{nn'}$ and Δr^i_n in the evaluation of the terms appearing in the expansion for β_{ijk} in Eq. (2).

The semiempirical method chosen was the well-known CNDO method[43] as modified by del Bene and Jaffe[44] and later by Lipari and Duke.[45] This particular parametrization, in addition to being a simple and direct numerical procedure, was chosen for its accurate description of both photoemission and ultraviolet absorption spectra of benzene. Furthermore, the model relies on only a few empirically adjustable input parameters. In this approximation the overlap matrix $S_{\mu\nu}$ is replaced by the unit matrix in the solution of Eq. (5). Furthermore, three- and four-center elec-

tron-repulsion integrals are neglected and the remaining integrals are reduced to an average electron repulsion between atoms:

$$(\mu\nu|\lambda\sigma) \simeq \delta_{\mu\nu}\delta_{\lambda\sigma}(\mu\mu|\lambda\lambda), \quad (\mu\mu|\lambda\lambda) \simeq \gamma_{AB}, \quad (12)$$

where $A(B)$ is the atom on which atomic orbital $\mu(\lambda)$ is centered. γ_{AB} is evaluated by means of the Mataga-Nishimoto expression,[46] in which the intra-atomic Coulomb repulsion integrals γ_{AA} were empirically determined. If penetration integrals are also neglected, the resulting equations stating the CNDO approximation are

$$\sum_{\nu} (F_{\mu\nu} - \epsilon_i \delta_{\mu\nu}) c_{\nu i} = 0, \quad (13)$$

$$F_{\mu\mu} = U_{\mu\mu} + (P_{AA} - \tfrac{1}{2}P_{\mu\mu})\gamma_{AA} + \sum_{B\neq A} (P_{BB} - Z_B)\gamma_{AB}, \quad (14a)$$

$$F_{\mu\nu} = H_{\mu\nu} - \tfrac{1}{2}P_{\mu\nu}\gamma_{AB}, \quad \mu \neq \nu. \quad (14b)$$

In the expression for $F_{\mu\mu}$, orbital μ is centered on atom A, and Z_A is the core charge on atom A. Also,

$$P_{BB} = \sum_{\substack{\lambda \\ \text{centered on} \\ \text{atom B}}} P_{\lambda\lambda} \quad (15)$$

is the net electron population on atom B. $U_{\mu\mu}$ is a core Hamiltonian matrix element for an electron in orbital μ and is given by

$$U_{\mu\mu} = I_{\mu} - (Z_A - 1)\gamma_{AA}, \quad (16)$$

where I_{μ} is the valence-state ionization energy for atomic orbital μ. The final quantities to be defined are the off-diagonal core Hamiltonian matrix elements $H_{\mu\nu}$. They are given by the Pople-Segal expression

$$H_{\mu\nu} = -\tfrac{1}{2}(\beta_{\mu} + \beta_{\nu})S_{\mu\nu}, \quad (17)$$

where $S_{\mu\nu}$ is the overlap integral between μ and ν, and $\beta_{\mu}(\beta_{\nu})$ is a hopping integral which refers to the atom on which $\mu(\nu)$ is centered. del Bene and Jaffe[44] distinguished between σ and π bonding by using different β values for σ and π interactions. Recently the CNDO method was further modified by Lipari and Duke[45] who used β_s and β_p to represent hopping between sites centered with s and p atomic orbitals, respectively. Furthermore, in this modification the Slater orbital exponent ζ is also empirically adjusted.

The complete set of empirical parameters then consists of valence-state ionization energies (I), hopping (resonance) integrals (β), Coulomb repulsion integrals (γ), and Slater orbital exponents (ζ). The input parameters were systematically adjusted for the two monosubstituted benzene derivatives, aniline and nitrobenzene (Fig. 1), to describe the photoemission data and ultraviolet absorption spectra, and quantitatively agree with the molecular second-order susceptibilities. The final set of input parameters for aniline and nitrobenzene was then used without further modification in the calculations for the photoemission data, ultraviolet absorption spectrum, and molecular second-order susceptibility of p-nitroaniline (Fig. 1).

It was found that the results of the adjustment procedure were particularly sensitive to the degree of electron localization on the individual substituent groups. The spatial extent of the molecular orbitals was carefully studied by systematically varying the orbital exponents: ζ: 2.50 Å^{-1} $\leq \zeta_{NH_2}(N) \leq 3.70$ Å^{-1}, $2.50 \leq \zeta_{NO_2}(N) \leq 4.60$, $3.44 \leq \zeta_{NO_2}(O) \leq 5.16$; and the hopping integrals β: 23 eV $\leq \beta_{NH_2}(N2s) \leq 28$ eV, $18 \leq \beta_{NH_2}(N2p) \leq 23$, $23 \leq \beta_{NO_2}(N2s) \leq 30$, $18 \leq \beta_{NO_2}(N2p) \leq 25$, $25 \leq \beta_{NO_2}(O2s) \leq 31$, $20 \leq \beta_{NO_2}(O2p) \leq 26$. For example, an increased $\zeta(\beta)$ results in an increased (decreased) electron localization through a decrease (increase) in the magnitude of the off-diagonal core Hamiltonian matrix element $H_{\mu\nu}$ defined above. The final choices for the input parameters are listed in Table I. The parameters used for benzene ring atoms were taken as originally reported.[45]

The calculations were performed for a fixed geometry of the molecules. A regular benzene ring was assumed for all systems. The remaining bond lengths and bond angles were obtained from reported x-ray structural and spectroscopic studies.[47-50] Cartesian coordinates were chosen for each system so that the benzene ring lies in the x-y plane, with the substituent nitrogen atoms placed on the x axis. Nitrobenzene and p-nitroaniline possess planar structures and so are members of the C_{2v} point group. Aniline, however, is nonplanar (bent) in its ground state.[47,48] The NH_2 hydrogens are elevated above the plane of the benzene ring, resulting in a 46° angle between the ring plane and that containing the NH_2 group. The symmetry of bent aniline is C_s. Calculations were performed on both planar and bent

TABLE I. Input parameters.

Parameter	C	H	N_{NH2}	N_{NO2}	O
ζ (Å^{-1})	3.78	2.30	3.03	3.03	4.10
β_s (eV)	20.0	10.0	25.0	23.0	25.0
β_p (eV)	17.0	···	20.0	18.0	20.0
γ (eV)	10.6	12.8	12.4	12.4	13.1
I_s (eV)	21.3	13.6	27.5	27.5	35.5
I_p (eV)	11.5	···	14.3	14.3	17.9

TABLE II. One-electron eigenvalues.

Aniline (Planar)		Aniline (Bent)		Nitrobenzene		*p*-nitroaniline	
Level	Energy (eV)	Level	Energy (eV)	Level	Energy (eV)	Level	Energy (eV)
26	3.38 $b_2(\sigma)$	26	3.35 $b_2(\sigma)$	31	1.50 $a_1(\sigma)$	34	1.70 $a_1(\sigma)$
25	2.86 $a_1(\sigma)$	25	2.89 $a_1(\sigma)$	30	1.17 $b_1(\pi)$	33	1.34 $b_1(\pi)$
24	1.96 $a_1(\sigma)$	24	1.98 $a_1(\sigma)$	29	1.00 $b_2(\sigma)$	32	1.09 $b_2(\sigma)$
23	1.93 $b_1(\pi)$	23	1.88 $b_1(\pi)$	28	0.70 $a_1(\sigma)$	31	0.96 $a_1(\sigma)$
22	1.87 $b_2(\sigma)$	22	1.87 $b_2(\sigma)$	27	−0.20 $a_1(\sigma)$	30	0.11 $a_1(\sigma)$
21	1.06 $a_1(\sigma)$	21	1.07 $a_1(\sigma)$	26	−0.51 $b_1(\pi)$	29	−0.24 $b_1(\pi)$
20	−0.41 $b_1(\pi)$	20	−0.51 $b_1(\pi)$	25	−1.45 $a_2(\pi)$	28	−1.36 $a_2(\pi)$
19	−0.71 $a_2(\pi)$	19	−0.71 $a_2(\pi)$	24	−2.53 $b_1(\pi)$	27	−2.26 $b_1(\pi)$
18	−8.91 $b_1(\pi)$	18	−9.14 $b_1(\pi)$	23	−10.73 $a_2(\pi)$	26	−9.60 $b_1(\pi)$
17	−10.00 $a_2(\pi)$	17	−10.00 $a_2(\pi)$	22	−10.93 $b_1(\pi)$	25	−10.74 $a_2(\pi)$
16	−12.19 $b_2(\sigma)$	16	−12.20 $b_2(\sigma)$	21	−12.06 $a_1(\sigma)$	24	−11.88 $a_1(\sigma)$
15	−12.35 $a_1(\sigma)$	15	−12.26 $a_1(\sigma)$	20	−12.60 $a_2(\pi)$	23	−12.26 $a_2(\pi)$
14	−12.47 $b_1(\pi)$	14	−12.73 $b_1(\pi)$	19	−12.80 $b_2(\sigma)$	22	−12.55 $b_2(\sigma)$
13	−14.95 $b_2(\sigma)$	13	−14.96 $b_2(\sigma)$	18	−13.26 $b_2(\sigma)$	21	−13.05 $b_2(\sigma)$
12	−15.31 $b_2(\sigma)$	12	−15.08 $a_1(\sigma)$	17	−14.04 $a_1(\sigma)$	20	−13.15 $b_1(\pi)$
11	−15.35 $a_1(\sigma)$	11	−15.30 $b_2(\sigma)$	16	−14.30 $b_1(\pi)$	19	−14.21 $a_1(\sigma)$
10	−15.41 $b_1(\pi)$	10	−15.92 $b_1(\pi)$	15	−15.90 $b_2(\sigma)$	18	−15.24 $b_2(\sigma)$
9	−17.61 $a_1(\sigma)$	9	−17.62 $a_1(\sigma)$	14	−16.21 $b_2(\sigma)$	17	−15.84 $b_2(\sigma)$
8	−19.05 $b_2(\sigma)$	8	−19.11 $b_2(\sigma)$	13	−17.12 $a_1(\sigma)$	16	−16.77 $b_1(\pi)$
7	−19.61 $a_1(\sigma)$	7	−19.50 $a_1(\sigma)$	12	−18.36 $b_2(\sigma)$	15	−16.91 $a_1(\sigma)$
6	−23.63 $a_1(\sigma)$	6	−23.46 $a_1(\sigma)$	11	−18.92 $a_1(\sigma)$	14	−17.43 $b_2(\sigma)$
5	−24.31 $b_2(\sigma)$	5	−24.39 $b_2(\sigma)$	10	−20.65 $a_1(\sigma)$	13	−19.25 $a_1(\sigma)$
4	−28.90 $a_1(\sigma)$	4	−28.67 $a_1(\sigma)$	9	−21.06 $b_1(\pi)$	12	−20.18 $b_1(\pi)$
3	−30.20 $b_2(\sigma)$	3	−30.24 $b_2(\sigma)$	8	−22.19 $a_1(\sigma)$	11	−20.26 $b_2(\sigma)$
2	−34.42 $a_1(\sigma)$	2	−34.47 $a_1(\sigma)$	7	−24.50 $b_2(\sigma)$	10	−20.42 $a_1(\sigma)$
1	−39.40 $a_1(\sigma)$	1	−39.90 $a_1(\sigma)$	6	−26.48 $a_1(\sigma)$	9	−22.00 $a_1(\sigma)$
				5	−30.86 $b_2(\sigma)$	8	−25.45 $b_2(\sigma)$
				4	−32.63 $a_1(\sigma)$	7	−26.28 $a_1(\sigma)$
				3	−37.16 $a_1(\sigma)$	6	−30.97 $b_2(\sigma)$
				2	−38.03 $b_2(\sigma)$	5	−31.14 $a_1(\sigma)$
				1	−48.13 $a_1(\sigma)$	4	−36.02 $a_1(\sigma)$
						3	−37.31 $b_2(\sigma)$
						2	−41.52 $a_1(\sigma)$
						1	−46.85 $a_1(\sigma)$

aniline. The planar calculation allowed C_{2v} symmetry assignments to be given to the wave functions. The results of the bent calculation were also assigned to representations of C_{2v} based on the similarity of the wave functions to those of the planar calculations.

In Table II are presented the molecular eigenvalues and the symmetry assignments of the molecular eigenfunctions of planar and bent aniline, nitrobenzene, and *p*-nitroaniline. All occupied and the eight lowest-energy virtual levels are shown for the four calculations. Along with the symmetry assignments, the σ or π character of each orbital is indicated.

The molecular eigenvalues of the calculations are related through Koopmans's theorem[51] to molecular ionization energies as measured with photoemission spectroscopy. Comparisons between calculated eigenvalues and ionization energies are shown in Figs. 2–4. The theoretical curves were obtained by placing a Gaussian distribution of width 0.2–0.4 eV upon each molecular eigenvalue. To allow for electron relaxation in the photoionization process, a constant was added to each eigenvalue. The constant was determined empirically by adjusting the eigenvalue of the highest occupied orbital to coincide with the first ionization peak. Inspection of the curves in Figs. 2 and 3 for aniline and nitrobenzene show satisfactory agreement between the calculated eigenvalues and the photoemission data.[52,53] In the case of *p*-nitroaniline the calculated curve in Fig. 4 provides a clear description of the photoemission curves.[54] In the important low-energy region, the peaks near 8.7, 9.8, and 11.0 eV represent the $b_1(\pi)$, $a_2(\pi)$, and $a_1(\sigma)$ levels, respectively. The oxygen lone pair $a_2(\pi)$ level along with the $b_2(\sigma)$ give rise to a doublet at 11.5 eV. In agreement with experimental statements[54] the structure appearing within the region between 9.8 and 11.0 eV probably represents vibrational structure.

Limited configuration-interaction (CI) calcula-

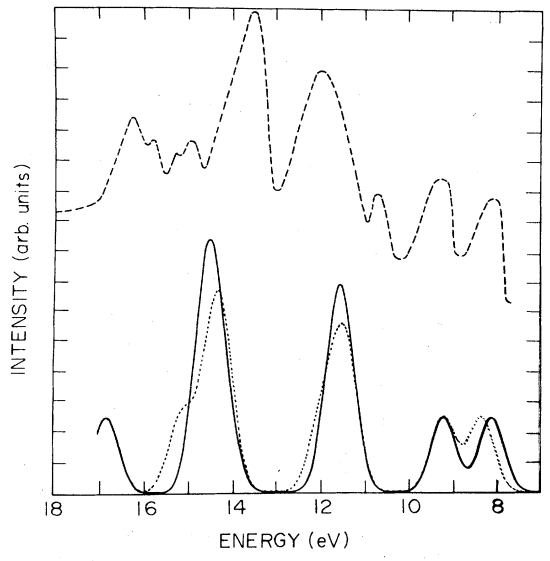

FIG. 2. Photoemission data for aniline (dashed); calculated one-electron eigenvalue spectra for planar (solid) and bent (dotted) aniline.

tions were carried out using the molecular orbitals and eigenvalues listed in Table II. All possible singly-excited aniline configurations involving the two highest occupied and the two lowest virtual molecular orbitals were mixed to yield the first four excited states for aniline. In nitrobenzene and *p*-nitroaniline three occupied and three virtual molecular orbitals were used in the CI calculation to form the first nine excited states. The calculated ground-to-excited-state transition energies and oscillator strengths for planar and bent aniline, nitrobenzene, and *p*-nitroaniline are presented in Tables III, IV, and V, respectively. Also listed are ultraviolet absorption data obtained in the vapor phase for the three molecules.[35,55-58] Comparison of the calculated and observed transition energies and oscillator strengths shows satisfactory agreement. This agreement is further illustrated for the case of *p*-nitroaniline[35] by Fig. 5. The compositions of the CI states are given in Tables III–V as linear combinations of singly-excited configurations. In the notation used for $\chi_{i\to j}$, i and j refer to the occupied and virtual levels, respectively, appearing in Table II.

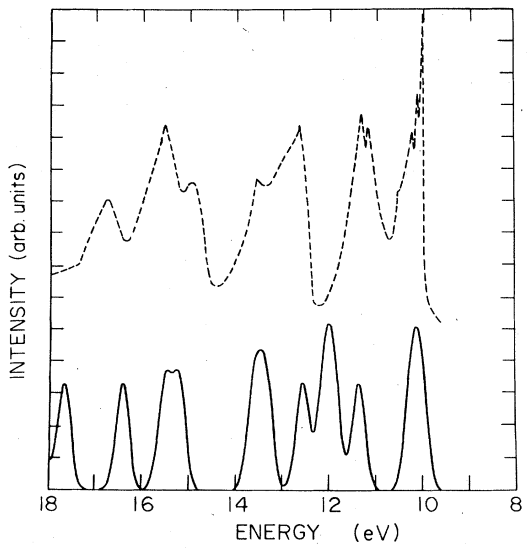

FIG. 3. Photoemission data for nitrobenzene (dashed); calculated one-electron eigenvalue spectrum for nitrobenzene (solid).

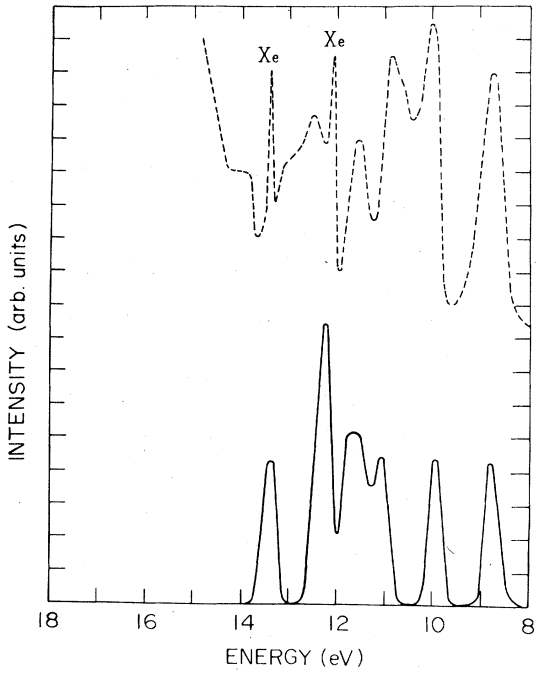

FIG. 4. Photoemission data for *p*-nitroaniline (dashed) (Xe represents the $^2P_{1/2}$ and $^2P_{3/2}$ lines of xenon); calculated one-electron eigenvalue spectrum for *p*-nitroaniline (solid).

IV. DISCUSSION

The excited-state energies and ground-to-excited-state transition moments listed above for each case were combined with the CI values for the dipole matrix elements $r^i_{nn'}$ and Δr^i_n to calculate the terms contained in the expansion of β_{ijk}. All components of β_{ijk} for each of the three cases were calculated, and the values of the nonzero components are given in Table VI. The calculations confirmed that since the molecules belong to the C_{2v} point group, all other components vanish by symmetry. Some components are present only for bent aniline since the C_{2v} symmetry is lowered in this system. The values listed in Table

TABLE III. Excitation energies and oscillator strengths for aniline.

Experimental [a]		Calculated Planar			Bent		
Energy (eV)	Oscillator strength	Symmetry	Energy (eV)	Oscillator strength	Composition	Energy (eV)	Oscillator strength	Composition
4.40	(0.028)	B_2	4.38	(0.048)	$0.87\chi_{18\to19} - 0.49\chi_{17\to20}$	4.47	(0.031)	$0.84\chi_{18\to19} + 0.54\chi_{17\to20}$
5.39	(0.144)	A_1	5.35	(0.175)	$0.94\chi_{18\to20} + 0.35\chi_{17\to19}$	5.46	(0.137)	$-0.92\chi_{18\to20} \pm 0.40\chi_{17\to19}$
6.40	(0.510)	B_2	6.47	(0.845)	$-0.87\chi_{17\to20} - 0.49\chi_{18\to19}$	6.50	(0.916)	$-0.84\chi_{17\to20} + 0.54\chi_{18\to19}$
6.88	(0.570)	A_1	6.51	(0.919)	$-0.94\chi_{17\to19} + 0.35\chi_{18\to20}$	6.53	(0.956)	$0.92\chi_{17\to19} + 0.40\chi_{18\to20}$

[a] K. Kimura and S. Nagakura, Mol. Phys. 9, 117 (1965).

VI are evaluated at the fundamental frequency 1.17 eV/$\hbar$, which corresponds to the 1.06-μ line of a Nd:YAG laser.

The results of the calculations can be compared with measurements from dc-induced second-harmonic generation (dc-SHG) in liquid solutions.[11,13,15,21,22,25] The measured quantity is the vector part of the molecular second-order susceptibility tensor and without Kleinman symmetry is given by the relation[59-62]

$$\beta_x = \beta_{xxx} + \tfrac{1}{3}\sum_{i\neq x}(\beta_{xii} + 2\beta_{iix}), \tag{18}$$

where the x axis remains aligned along the dipolar axis of the molecule. A discussion of the vector nature of β_x appears in the Appendix. Table VII shows the comparison between experimental[13,18,23] and calculated values of β_x for aniline, nitrobenzene, and p-nitroaniline. By symmetry β_x has the same sign as the ground-state dipole moment in each case.[10,13] The present calculations correctly predict the sign of β_x for these systems, and the calculated β_x values agree in magnitude with the measured quantities to within experimental uncertainty. The calculated β_x value for p-nitroaniline is compared with the experimental result measured in nonpolar *trans*-stilbene by Levine and Bethea[18] since p-nitroaniline is subject to strong polar solvent effects.[57,63] We have separately observed by these calculations that such effects can significantly alter the electronic structure of p-nitroaniline, resulting in marked enhancement of β_x.

In the calculation of β_x for each case, the β_{xxx} component is the major contribution (Table VI). Moreover, only those excited states that transform as the A_1 representation of the C_{2v} point group are symmetry allowed in the determination of β_{xxx}. The x operator is isomorphic to the A_1 representation of the group C_{2v}. Thus dipole coupling may occur between states of the same symmetry since A_1 is the totally symmetric representation. In the perturbation expansion for β_{ijk} every term consists of a product in which at least one factor is a dipole coupling to the ground state, which is also totally symmetric. Hence any two excited states n and n' in an arbitrary term for β_{xxx} must both be of A_1 symmetry.

The remaining components β_{xyy}, β_{yyx}, β_{xzz}, and β_{zzx} contained in β_x are smaller than β_{xxx} because the dipole moment difference between ground and excited state, $\Delta\vec{r}_n$, which is an important quantity in determining β_{ijk}, has no y or z component because of C_{2v} symmetry. Only off-diagonal dipole moment matrix elements and transition moments continue to contribute to the components of

TABLE IV. Excitation energies and oscillator strengths for nitrobenzene.

Experimental [a] Energy (eV)	Experimental [a] Oscillator strength	Calculated Symmetry	Calculated Energy (eV)	Calculated Oscillator strength	Calculated Composition
		B_1	4.26	(0.0007)	$0.93\chi_{21\to24} + 0.38\chi_{21\to26}$
4.38	(0.01)	B_2	4.49	(0.042)	$0.83\chi_{23\to24} - 0.52\chi_{22\to25} - 0.19\chi_{23\to26}$
5.11	(0.17)	A_1	5.28	(0.344)	$0.96\chi_{22\to24} + 0.27\chi_{23\to25} + 0.05\chi_{22\to26}$
6.42	(0.38)	B_2	6.17	(0.351)	$0.68\chi_{22\to25} + 0.54\chi_{23\to24} + 0.49\chi_{23\to26}$
		A_1	6.35	(0.696)	$-0.92\chi_{23\to25} + 0.31\chi_{22\to26} + 0.24\chi_{22\to24}$
		A_2	6.82	(0.0)	$1.00\chi_{21\to25}$
		B_1	7.05	(0.0)	$-0.93\chi_{21\to26} + 0.38\chi_{21\to24}$
7.56	(0.87)	B_2	7.07	(0.683)	$0.85\chi_{23\to26} - 0.51\chi_{22\to25} - 0.12\chi_{23\to24}$
		A_1	7.35	(0.240)	$0.95\chi_{22\to26} - 0.29\chi_{23\to25} + 0.13\chi_{22\to24}$

[a] S. Nagakura, M. Kojima, and Y. Maruyama, J. Mol. Spectrosc. 13, 174 (1964).

β_{ijk} involving y or z. Inspection of the intermediate results of the calculation for each system reveal that these off-diagonal terms are always relatively small.

The correlation diagram for aniline, nitrobenzene, and p-nitroaniline is presented in Fig. 6 to illustrate the important one-electron molecular levels that contribute to the A_1-state configurations in each case. For aniline, the A_1 states determining β_{xxx} are located at 5.35 and 6.51 eV and primarily consist of the respective configurations $\chi_{17\to19}$ and $\chi_{18\to20}$. The one-electron levels 17, 19, and 20 are $a_2(\pi)$, $a_2(\pi)$, and $b_1(\pi)$ levels, respectively, that are nearly identical to the corresponding $a_2(\pi)$ and $b_1(\pi)$ benzene levels contained in the doubly degenerate $e_{1g}(\pi)$ and $e_{2u}(\pi)$ sets. The occupied level 18 is a particularly important $b_1(\pi)$ level in that it is a combined benzene-ring–NH_2-substituent-group level whose eigenfunction has a relatively large amplitude on the NH_2 group. The $b_1 \to b_1$ configuration $\chi_{18\to20}$ has a calculated larger dipole moment change from the ground state than the $a_2 \to a_2$ configuration $\chi_{17\to19}$. From Eq. (9c) the diagonal components $\Delta x_{i\to j}$ for this difference are given by

$$\Delta x_{i\to j} = \langle \chi_{i\to j} | M^x | \chi_{i\to j} \rangle - \langle \Psi_g | M^x | \Psi_g \rangle = m^x_{jj} - m^x_{ii}. \tag{19}$$

We find for aniline that $\Delta x_{18\to20} = 2.1$ D while

TABLE V. Excitation energies and oscillator strengths for p-nitroaniline.

Experimental Energy (eV)	Experimental Oscillator strength	Calculated Symmetry	Calculated Energy (eV)	Calculated Oscillator strength	Calculated Composition
		B_1	4.20	(0.0004)	$-0.93\chi_{24\to27} - 0.37\chi_{24\to29}$
4.35 [a] (3.85) [b]	(0.64) [c]	A_1	4.37	(0.493)	$-0.98\chi_{26\to27} - 0.17\chi_{25\to28} + 0.06\chi_{26\to29}$
		B_2	4.38	(0.012)	$-0.81\chi_{26\to28} + 0.54\chi_{25\to27} - 0.22\chi_{25\to29}$
		B_2	5.57	(0.394)	$-0.84\chi_{25\to27} - 0.54\chi_{26\to28} - 0.07\chi_{25\to29}$
5.73		A_1	6.14	(0.089)	$-0.87\chi_{26\to29} + 0.48\chi_{25\to28} - 0.13\chi_{26\to27}$
		A_1	6.63	(0.726)	$0.86\chi_{25\to28} + 0.49\chi_{26\to29} - 0.12\chi_{26\to27}$
		A_2	6.80	(0.0)	$1.00\chi_{24\to28}$
		B_2	7.06	(0.303)	$0.97\chi_{25\to29} - 0.22\chi_{26\to28} + 0.07\chi_{25\to27}$
		B_1	7.49	(0.0)	$-0.93\chi_{24\to29} + 0.37\chi_{24\to27}$

[a] F. Bertinelli, P. Palmieri, A. Brilliante, and C. Taliani, Chem. Phys. 25, 333 (1977) (Vapor Phase).

[b] J. F. Corbett, Spectrochim. Acta 23A, 2315 (1967) (n-hexane solution).

[c] V. I. Danilova and Yu. P. Morozova, Opt. Spectrosc. 12, 5 (1962) (n-hexane solution).

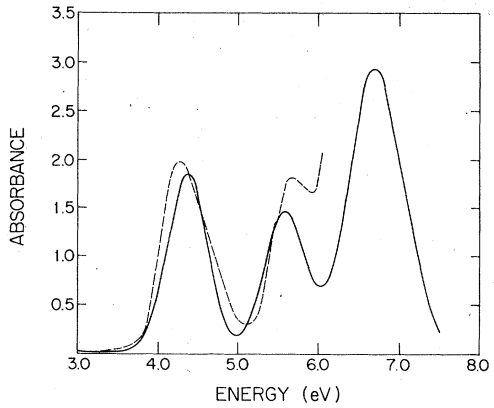

FIG. 5. Ultraviolet absorption data for p-nitroaniline (dashed); calculated excitation spectrum for p-nitroaniline (solid).

$\Delta x_{17\to19} = 0.4$ D. Comparison of the corresponding MO diagrams given in Figs. 7 and 8 illustrates how the larger value for $\Delta x_{18\to20}$ arises from redistribution of electron density away from the NH_2 nitrogen site into the benzene ring. In contrast, only minor changes occur along the x axis between ψ_{17} and ψ_{19}, accounting for the relatively small value of $\Delta x_{17\to19}$.

Of the remaining components only β_{xyy} and β_{yyx} combine with β_{xxx} in determining β_x. Components of β_{ijk} involving z, such as β_{xzz} and β_{zzx}, vanish identically in aniline. Since there are no aniline excited states of B_1 symmetry, no dipole coupling to the z operator can occur. Furthermore, as described above, components of β_{ijk} involving y or z are smaller than β_{xxx}, and for aniline β_{xyy} and β_{yyx} together constitute less than one fourth of the total value of β_x.

In the case of nitrobenzene, the A_1 states most important to β_{xxx} are located at 5.28 and 6.35 eV. These states are composed primarily of the two configurations $\chi_{22\to24}$ and $\chi_{23\to25}$, respectively. The one-electron levels 23 and 25 are ringlike $a_2(\pi)$ levels very similar to their counterparts in both aniline and benzene, and the occupied $b_1(\pi)$ level 22 corresponds to the $b_1(\pi)$ level of benzene. Importantly, level 24 is a combined $b_1(\pi)$ level of benzene with a large contribution from the NO_2 group. This arrangement of $b_1(\pi)$ levels in nitrobenzene is reversed from that of aniline, where it is the occupied level 18 that is a combined benzene-ring–substituent-group level and the virtual level 20 that is essentially a benzene level. As in aniline, the $b_1 \to b_1$ configuration exhibits a dipole moment change from the ground state, $\Delta x_{22\to24} = 3.9$ D, much larger than that for the $a_2 \to a_2$ configuration, $\Delta x_{23\to25} = 0.1$ D. Contour diagrams for the $b_1(\pi)$ molecular orbitals ψ_{22} and ψ_{24} given in Fig. 9 show that in this case the larger $\Delta x_{22\to24}$ results from transfer of electron density away from the benzene ring out onto the NO_2 substituent group. The corresponding diagrams for the $a_2(\pi)$ orbitals ψ_{23} and ψ_{25} in Fig. 10 exhibit no redistribution of electron density along the x axis, consistent with the smaller value for $\Delta x_{23\to25}$. The remaining nitrobenzene A_1 excited state at 7.35 eV, which is composed primarily of configuration $\chi_{22\to26}$, only contributes approximately 5% to the total value of β_{xxx}.

There is a minor 10% contribution to β_x from the components β_{xyy} and β_{yyx}. It is interesting to point out that the excited state of B_1 symmetry which determines β_{xzz} and β_{zzx} is composed of the nitrobenzene $n \to \pi^*$ configuration $\chi_{21\to24}$. The β_{xzz} and β_{zzx} components add a negligible 0.1% to β_x.

The features found important to β_{xxx} for aniline and nitrobenzene hold in the case of p-nitroaniline as well. The A_1 excited states composed of $b_1 \to b_1$ and $a_2 \to a_2$ configurations provide the major terms for β_{xxx}, and $b_1 \to b_1$ configurations exhibit a larger dipole moment change $\Delta x_{i\to j}$ than $a_2 \to a_2$ configurations. Moreover, reference to the correlation diagram of Fig. 6 shows that in the region containing the highest occupied and lowest empty one-electron levels, the level distribution and ordering for p-nitroaniline and nitrobenzene are nearly the same except for one important added feature. In addition to the first empty $b_1(\pi)$ level 27 being the combined benzene-ring–NO_2 level originating from nitrobenzene, the highest occupied $b_1(\pi)$ lev-

TABLE VI. Components of β_{ijk} in units of 10^{-30} cm^5/esu calculated at 1.17 eV (1.06 μ).

Component	Aniline (Planar)	Aniline (Bent)	Nitrobenzene	p-nitroaniline
XXX	1.221	0.899	−2.539	8.635
XYY	0.253	0.208	0.311	−1.328
XZZ	0.0	0.0	0.003	−0.004
XXZ	0.0	0.002	0.0	0.0
YYZ	0.427	0.322	0.192	−0.796
ZXX	0.0	0.002	0.0	0.0
ZYY	0.0	−0.001	0.0	0.0
ZZX	0.0	0.0	0.004	−0.005

TABLE VII. Comparison of calculated and experimental determinations of β_x in units of 10^{-30} cm^5/esu.

	Experimental ±15%	Calculated
Aniline	0.9 [a]	1.59 (planar)
	1.1 [b]	1.18 (bent)
Nitrobenzene	−2.0 [a]	−2.30
	−2.2 [b]	
p-nitroaniline	6.4 [c]	6.53

[a] B. F. Levine and C. G. Bethea, J. Chem. Phys. 63, 2666 (1975) (measured at 1.06 μ).

[b] J. L. Oudar and D. S. Chemla, J. Chem. Phys. 66, 2664 (1977) (measured at 1.06 μ).

[c] B. F. Levine and C. G. Bethea, J. Chem. Phys. 69, 5240 (1978) (measured at 1.3 μ).

el 26 is the combined benzene-ring–NH_2-group level from aniline. This special feature leads to highly asymmetric charge-separated states which dominate the calculations of β_{ijk} for *p*-nitroaniline.

Of the three *p*-nitroaniline A_1 states located at 4.37, 6.14, and 6.63 eV, the lowest energy state is composed primarily of $\chi_{26\to27}$. The two higher energy A_1 excited states at 6.14 and 6.63 eV consist mostly of the configurations $\chi_{25\to28}$ and $\chi_{26\to29}$, respectively. The levels 25 and 28 are the familiar ringlike $a_2(\pi)$ levels described above. Level 29 is similar to the $b_1(\pi)$ level 27, with an additional node between the NO_2 nitrogen and the ring.

The lowest-energy A_1 state of *p*-nitroaniline is responsible for almost the entire magnitude of β_{xxx}. In the calculation, the product $(x_{ng})^2\Delta x_n$, where x_{ng} is the transition dipole moment, occurs in the major terms for β_{xxx}. Inspection of the intermediate results shows that only the lowest-energy A_1 state yields relatively large values of both x_{ng} and Δx_n. As in the cases of aniline and nitrobenzene, the excited state consisting mostly of the $a_2 \to a_2$ configuration $\chi_{25\to28}$ has a characteristically low value for $\Delta x_{25\to28}$ (0.7 D) compared to the $b_1 \to b_1$-configuration-dominated states in which

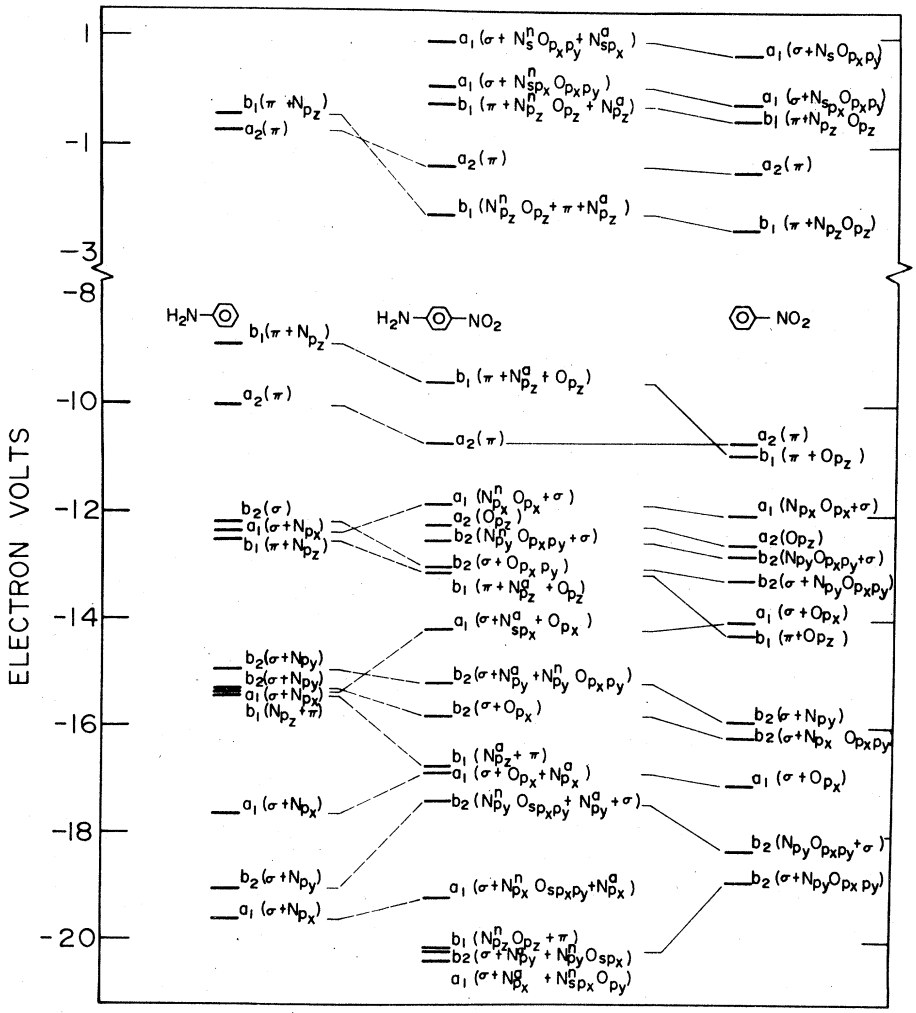

FIG. 6. Correlation diagram for one-electron eigenvalues for aniline, nitrobenzene, and *p*-nitroaniline. Atomic orbital contributions are given in order of percent contribution: for example, the b_1 levels of *p*-nitroaniline at −9.6 and −2.3 eV consist of 73% ring (π), 19% NH_2 (N^a_{pz}), and 7% NO_2 (O_{pz}); and 49% NO_2 ($N^n_{pz}O_{pz}$), 47% ring (π), and 4% NH_2 (N^a_{pz}), respectively.

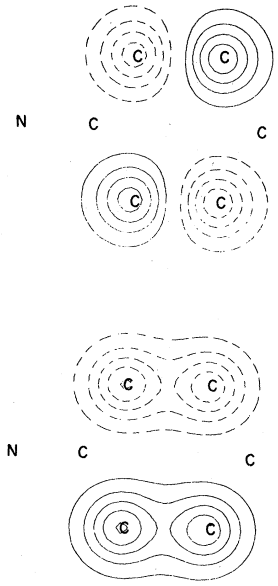

FIG. 7. Contour diagrams of molecular orbitals 17 (bottom) and 19 (top) of aniline drawn in the plane $z = 0.6$ Å. Positive and negative values are indicated by solid and dashed lines, respectively. Outermost contour lines have a magnitude of 0.1, with successive lines increasing (decreasing for negative contours) by 0.1 increments toward atomic sites.

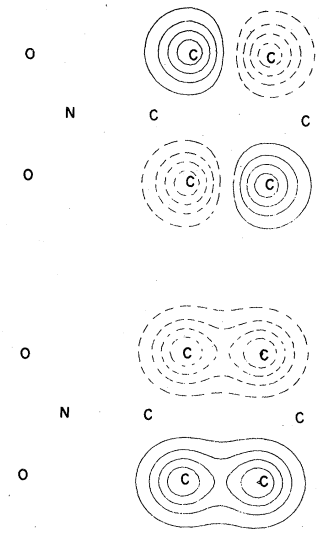

FIG. 9. Contour diagrams of molecular orbitals 23 (bottom) and 25 (top) of nitrobenzene drawn in the plane $z = 0.6$ Å. Positive and negative values are indicated by solid and dashed lines, respectively. Outermost contour lines have a magnitude of 0.1, with successive lines increasing (decreasing for negative contours) by 0.1 increments toward atomic sites.

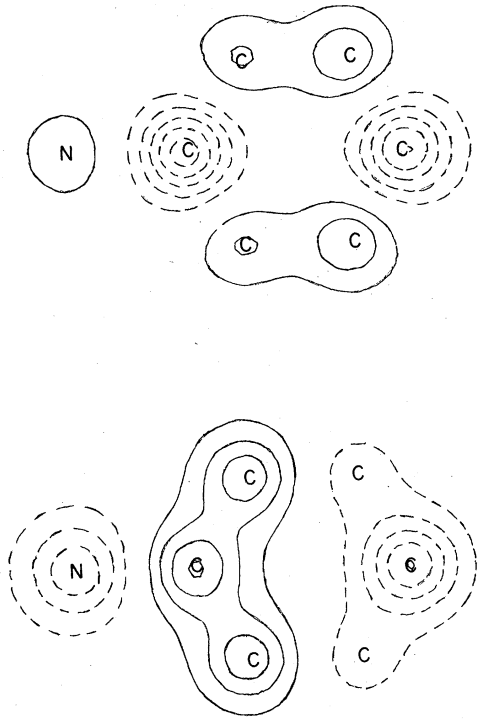

FIG. 8. Contour diagrams of molecular orbitals 18 (bottom) and 20 (top) of aniline drawn in the plane $z = 0.6$ Å. Positive and negative values are indicated by solid and dashed lines, respectively. Outermost contour lines have a magnitude of 0.1, with successive lines increasing (decreasing for negative contours) by 0.1 increments toward atomic sites.

$\Delta x_{26\to 27} = 6.5$ D and $\Delta x_{26\to 29} = 3.6$ D. However, only the lowest-energy A_1 state also possesses a large transition dipole moment: $x_{26\to 27,g} = 4.4$ D in contrast with $x_{26\to 29,g} = 0.9$ D.

These results are clearly illustrated by the following contour diagrams. Figure 11 for ψ_{26} and ψ_{27} clearly shows that in the configuration $\chi_{26\to 27}$ electron density is transferred from the region of the NH_2 group across the ring to the NO_2 group and its neighboring carbon sites. In Figs. 12 and 13 contour plots are drawn for the two functions $(\psi_{26})^2 - (\psi_{27})^2$ and $(\psi_{26})(\psi_{27})$, which are related to $\Delta x_{26\to 27}$ and $x_{26\to 27,g}$, respectively:

$$\Delta x_{26\to 27} = -\int [(\psi_{26})^2 - (\psi_{27})^2] x\, dx\,,$$
$$x_{26\to 27,g} = \sqrt{2} \int (\psi_{26})(\psi_{27}) x\, dx\,. \tag{20}$$

Each function exhibits a marked asymmetric distribution across the entire length of the p-nitroaniline molecule. This is evidenced by the positive value of these functions in the vicinity of the NH_2 group and the negative values located on the NO_2 group. Accordingly, the first moments associated with x appearing in the Eqs. (20) yield relatively large values of $\Delta x_{26\to 27}$ and $x_{26\to 27,g}$.

The asymmetry of the product functions along the x axis which characterizes $\chi_{26\to 27}$ is not present in the configurations composing the other A_1 states, for example, $\chi_{25\to 28}$. The functions $(\psi_{25})^2$

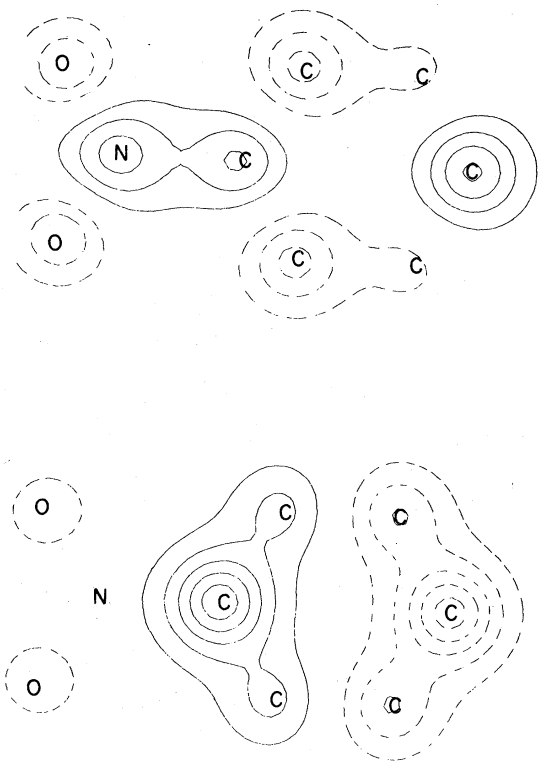

FIG. 10. Contour diagrams of molecular orbitals 22 (bottom) and 24 (top) of nitrobenzene drawn in the plane $z = 0.6$ Å. Positive and negative values are indicated by solid and dashed lines, respectively. Outermost contour lines have a magnitude of 0.1, with successive lines increasing (decreasing for negative contours) by 0.1 increments toward atomic sites.

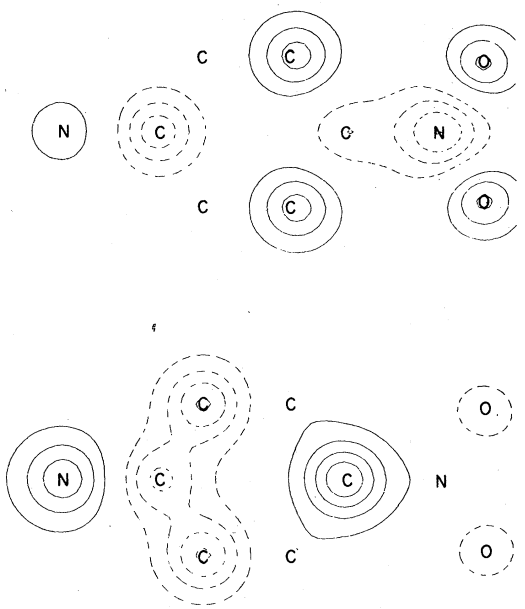

FIG. 11. Contour diagrams of molecular orbitals 26 (bottom) and 27 (top) of p-nitroaniline drawn in the plane $z = 0.6$ Å. Positive and negative values are indicated by solid and dashed lines, respectively. Outermost contour lines have a magnitude of 0.1, with successive lines increasing (decreasing for negative contours) by 0.1 increments toward atomic sites.

$-(\psi_{28})^2$ and $(\psi_{25})(\psi_{28})$ are plotted as contour diagrams in Figs. 14 and 15. The combination $(\psi_{25})(\psi_{28})$ exhibits an asymmetry along the x axis, resulting in a large value for $x_{25\rightarrow 28,g}$. In contrast, $(\psi_{25})^2 - (\psi_{28})^2$ is nearly symmetrical along the x axis, resulting in a small value of $\Delta x_{25\rightarrow 28}$.

In addition to β_{xxx}, β_{xyy}, and β_{yyx} contribute 13% to β_x in p-nitroaniline while β_{xzz} and β_{zzx} have virtually no effect on β_x, constituting 0.05% of the total. As in nitrobenzene, the B_1 excited state in p-nitroaniline which is responsible for β_{xzz} and β_{zzx} is composed of an $n \rightarrow \pi^*$ configuration $\chi_{24\rightarrow 27}$.

The bond-additivity approximation[13,14,20,23,64-66] assumes that β_x for p-nitroaniline is a vector sum of the measured β_x values for aniline and nitrobenzene. The apparent difference between the bond-additivity result and the observed value of β_x for p-nitroaniline has been ascribed to an additional term due to intramolecular charge transfer.[14,23] The results of our calculations demonstrate how this approach exceeds the limits of the approximation. The A_1 excited states which are primarily responsible for β_x values for aniline and nitrobenzene have no counterparts in p-nitroaniline. For example, reference to the correlation diagram of Fig. 6 shows that the $b_1(\pi)$ levels 20 of aniline and 22 of nitrobenzene, necessary to their respective A_1 excited states, are completely absent in p-nitroaniline. Rather, as described above, β_x for p-nitroaniline is determined by an A_1 excited state that is unique to this system and contains no contributions which derive from the hyperpolarizabilities of either aniline or nitrobenzene.

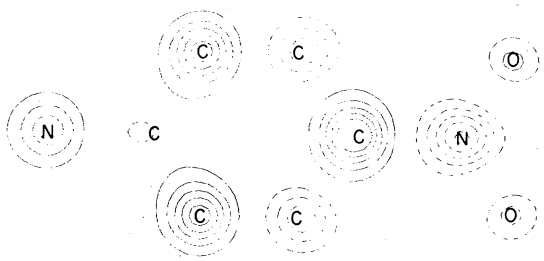

FIG. 12. Contour diagram of the product function $(\psi_{26})^2 - (\psi_{27})^2$ of p-nitroaniline drawn in the plane $z = 0.6$ Å. Positive and negative values are indicated by solid and dashed lines, respectively. Outermost contour lines have a magnitude of 0.03, with successive lines increasing (decreasing for negative contours) by 0.03 increments toward atomic sites.

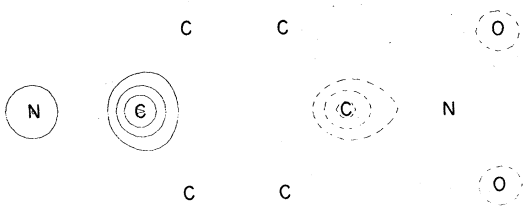

FIG. 13. Contour diagram of the product function $(\psi_{26})(\psi_{27})$ of p-nitroaniline drawn in the plane $z = 0.6$ Å. Positive and negative values are indicated by solid and dashed lines, respectively. Outermost contour lines have a magnitude of 0.03, with successive lines increasing (decreasing for negative contours) by 0.03 increments toward atomic sites.

The frequency dependence for each nonzero β_{ijk} tensor component is shown in Figs. 16, 17, and 18 for planar aniline, nitrobenzene, and p-nitroaniline, respectively. In the low-frequency region ($\omega \sim 0.8$ eV/$\hbar$) each curve exhibits relatively small dispersion and correspondingly the Kleinman symmetry conditions[38] $\beta_{xyy} = \beta_{yyx}$ are satisfied. Above 0.8 eV/$\hbar$ the Kleinman relations begin to break down in each case, and importantly at the Nd:YAG laser frequency 1.17 eV/$\hbar$ (1.06μ) β_{xyy} differs appreciably from β_{yyx}. However, assuming Kleinman symmetry at this frequency, which is common practice, leads to β_x values differing by only 10%. As 2ω approaches the first excitation frequency ($\omega_{ng} \sim 4$ eV/$\hbar$), each component begins to diverge widely. Finally, Fig. 19 compares the dispersion of β_x for aniline, nitrobenzene, and p-nitroaniline.

V. CONCLUSION

We have presented a successful calculational procedure for determining molecular second-order susceptibilities. Analysis of their microscopic origin provides a direct means for understanding the macroscopic nonlinear optical response in organic molecular solids. The particular molecular units considered here are model systems for those classes of organic solids which have already been observed to possess exceptional nonlinear optical properties.

The important excited states of aniline, nitrobenzene, and p-nitroaniline have been identified and examined in their relationship with the molecular second-order susceptibility tensor components β_{ijk}. The detailed nature of the charge separation accompanying these states has been discussed in terms of both the configurations composing the excited states, and also the one-electron molecular orbitals which determine those configurations. These results demonstrate that the bond-additivity approximation is inappropriate for p-nitroaniline. Finally, the frequency dependence of the β_{ijk} components in each case shows that the Kleinman relations are valid approximations only at relatively low frequencies.

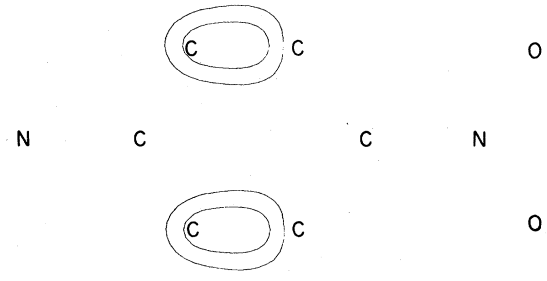

FIG. 14. Contour diagram of the product function $(\psi_{25})^2 - (\psi_{28})^2$ of p-nitroaniline drawn in the plane $z = 0.6$ Å. Positive and negative values are indicated by solid and dashed lines, respectively. Outermost contour lines have a magnitude of 0.03, with successive lines increasing (decreasing for negative contours) by 0.03 increments toward atomic sites.

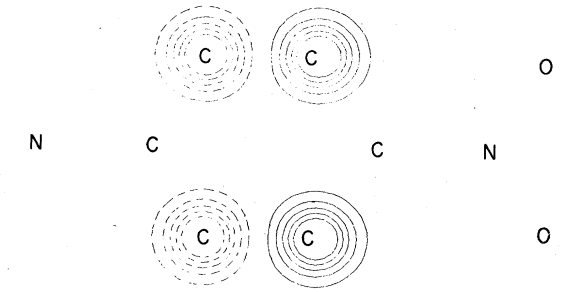

FIG. 15. Contour diagram of the product function $(\psi_{25})(\psi_{28})$ of p-nitroaniline drawn in the plane $z = 0.6$ Å. Positive and negative values are indicated by solid and dashed lines, respectively. Outermost contour lines have a magnitude of 0.03, with successive lines increasing (decreasing for negative contours) by 0.03 increments toward atomic sites.

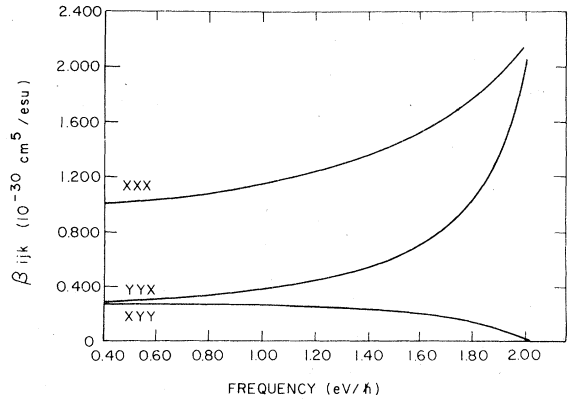

FIG. 16. Frequency dependence of β_{xxx}, β_{xyy}, and β_{yyx} of aniline.

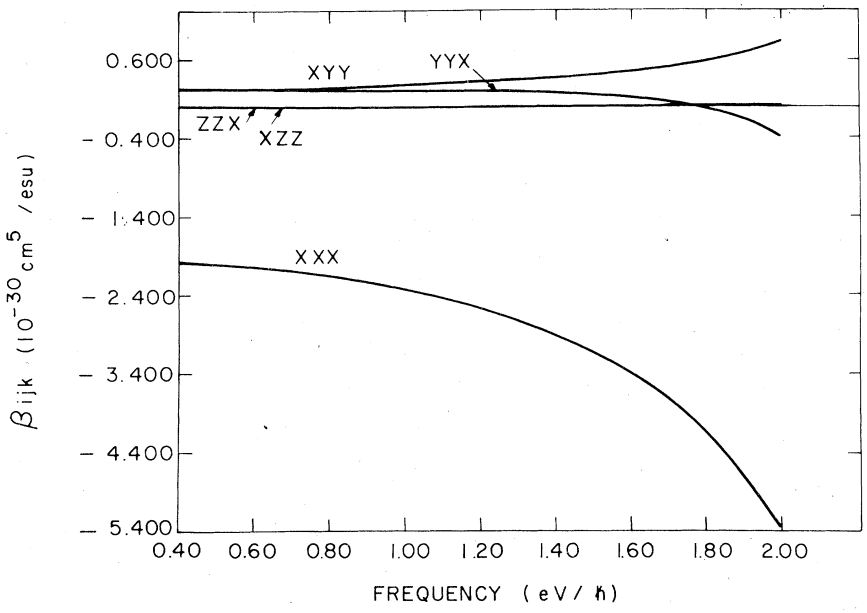

FIG. 17. Frequency dependence of β_{xxx}, β_{xyy}, β_{yyx}, β_{xzz}, and β_{zzx} of nitrobenzene.

Current studies of organic solids and single-crystal polymers are being carried out by having extended these calculations to other molecular and polymer chain systems.

ACKNOWLEDGMENTS

We would like to thank K. D. Singer, G. F. Lipscomb, Z. Levine, and M. Merlin for many helpful discussions in the preparation of this work. Valuable assistance in computing was provided by R. Marshall and R. Warburton. C. B. Duke and A. Paton were helpful in providing copies of their CNDO computer program which was utilized in the early stages of this work. This work was supported by the NSF MRL Program under Grant No. DMR 76-80994 and by DARPA under Grant No. DAAK 0045.

APPENDIX

In measuring hyperpolarizabilities of molecules in solution, the relevant quantity measured, after averaging over molecular orientation, is[60]

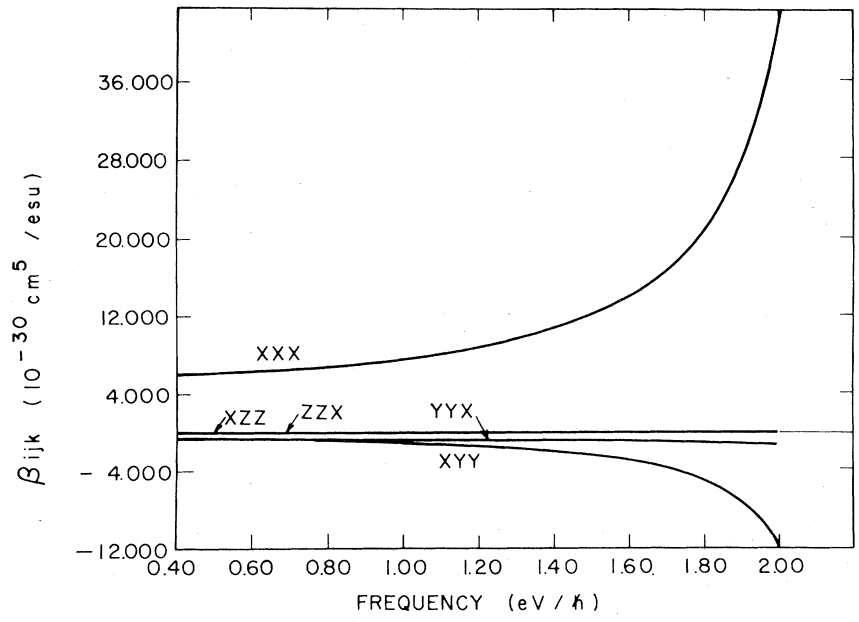

FIG. 18. Frequency dependence of β_{xxx}, β_{xyy}, β_{yyx}, β_{xzz}, and β_{zzx} of *p*-nitroaniline.

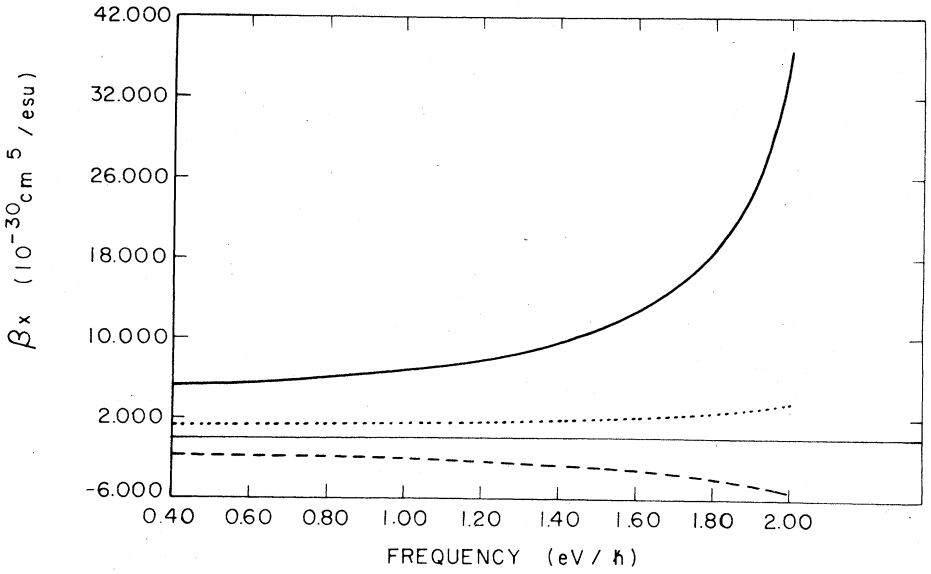

FIG. 19. Frequency dependence of β_x of planar aniline (dotted), nitrobenzene (dashed), and p-nitroaniline (solid).

$$\beta_{iij}\mu_j+\beta_{iji}\mu_j+\beta_{jii}\mu_j\,, \tag{A1}$$

where repeated indices are summed over and μ_j is the jth component of the molecular ground-state dipole moment $\vec{\mu}$. This can be re-expressed as $\vec{\beta}\cdot\vec{\mu}$ where $\vec{\beta}$ is the vector part of the third-rank tensor β_{ijk} defined as

$$\beta_k\equiv\tfrac{1}{3}(\beta_{knm}\delta_{nm}+\beta_{nkm}\delta_{nm}+\beta_{nmk}\delta_{nm})\,; \tag{A2}$$

a particular component, say $k=1$ (or x), becomes

$$\beta_1=\tfrac{1}{3}(\beta_{111}+\beta_{122}+\beta_{133}+\beta_{111}+\beta_{212}+\beta_{313}+\beta_{111}+\beta_{221}+\beta_{331})\,. \tag{A3}$$

Second-harmonic-generation symmetry requires $\beta_{ijk}=\beta_{ikj}$, so that

$$\beta_1=\tfrac{1}{3}(3\beta_{111}+\beta_{122}+2\beta_{221}+\beta_{133}+2\beta_{331})$$

$$=\beta_{111}+\tfrac{1}{3}\sum_{j\neq1}(\beta_{1jj}+2\beta_{jj1})\,. \tag{A4}$$

By applying the transformation properties of third-rank tensors, one can show that the quantity β_k does indeed transform as a vector. Considering two coordinate systems, primed and unprimed, the transformation properties for a vector $\vec{V}$ are

$$V_i'=a_{ij}V_j\,, \tag{A5}$$

where the a_{ij} are the direction cosines between the coordinate systems and obey the orthogonality relations

$$a_{ij}a_{kj}=a_{ji}a_{jk}=\delta_{ik}\,. \tag{A6}$$

If β_k transforms as a vector, it must obey an equation of the form $\beta_k'=a_{kl}\beta_l$, which from Eq. (A2) results in

$$\beta_k'=\tfrac{1}{3}a_{kl}(\beta_{lnm}\delta_{nm}+\beta_{nlm}\delta_{nm}+\beta_{nml}\delta_{nm})\,. \tag{A7}$$

The right-hand side of Eq. (A7) now implies a summation over all indices in β_{lnm} so that all three terms above are equal, resulting in

$$\beta_k'=a_{kl}\delta_{nm}\beta_{lnm}\,. \tag{A8}$$

For the vector part of β_{ijk} in the primed coordinate system

$$\beta_k'=\tfrac{1}{3}(\beta_{knm}'\delta_{nm}+\beta_{nkm}'\delta_{nm}+\beta_{nmk}'\delta_{nm})\,. \tag{A9}$$

Next β_{ijk}' is expressed in terms of β_{ijk} through the tensor transformation relations

$$\beta_{ijk}'=a_{il}a_{jm}a_{kn}\beta_{lmn}\,. \tag{A10}$$

We then obtain for β_k' in terms of β_{ijk}:

$$\beta_k'=\tfrac{1}{3}(a_{ki}a_{nj}a_{ml}\beta_{ijl}\delta_{nm}+a_{ni}a_{kj}a_{ml}\beta_{ijl}\delta_{nm}+a_{ni}a_{mj}a_{kl}\beta_{ijl}\delta_{nm})\,. \tag{A11}$$

Since the products involving the a_{ij} commute, all three terms on the right-hand side of Eq. (A11) are equal, resulting in

$$\beta_k'=a_{ki}a_{nj}a_{nl}\beta_{ijl}\,, \tag{A12}$$

where the sum over m has been performed explicitly in each of the three terms by using the properties of the δ function. Furthermore, from the orthogonality relations one finds

$$\beta_k'=a_{ki}\delta_{jl}\beta_{ijl}\,, \tag{A13}$$

which is equivalent to Eq. (A8).

[1]S. K. Kurtz and T. T. Perry, J. Appl. Phys. 39, 3798 (1968).
[2]H. Bass, D. Bua, R. Mozzi, and R. M. Monchamp, Appl. Phys. Lett. 15, 393 (1969).
[3]L. D. Derkacheva, A. I. Krymona, and N. P. Sopina, JETP Lett. 11, 319 (1970).
[4]B. L. Davydov, L. D. Derkacheva, V. V. Dunina, M. E. Zhabotinskii, V. F. Zolin, L. G. Koreneva, and M. A. Samokhina, JETP Lett. 12, 16 (1970); Opt. Spectrosc. 30, 274 (1971).
[5]J. Jerphagnon, IEEE J. Quantum Electron. 7, 42 (1971).
[6]J. R. Gott, J. Phys. B 4, 116 (1971).
[7]P. D. Southgate and D. S. Hall, J. Appl. Phys. 43, 2765 (1972).
[8]J. G. Bergman, G. R. Crane, B. F. Levine, and C. G. Bethea, Appl. Phys. Lett. 20, 21 (1972).
[9]G. P. Bolognesi, S. Mezzetti, and F. Pandarese, Opt. Commun. 8, 268 (1973).
[10]B. F. Levine and C. G. Bethea, J. Chem. Phys. 60, 3865 (1974).
[11]B. F. Levine and C. G. Bethea, Appl. Phys. Lett. 24, 445 (1974).
[12]B. F. Levine, J. Chem. Phys. 63, 115 (1975).
[13]B. F. Levine and C. G. Bethea, J. Chem. Phys. 63, 2666 (1975).
[14]B. F. Levine, Chem. Phys. Lett. 37, 516 (1976).
[15]B. F. Levine and C. G. Bethea, J. Chem. Phys. 65, 1989 (1976).
[16]B. F. Levine and C. G. Bethea, J. Chem. Phys. 65, 2429 (1976); *ibid.* 65, 2439 (1976).
[17]B. F. Levine and C. G. Bethea, J. Chem. Phys. 66, 1070 (1977).
[18]B. F. Levine and C. G. Bethea, J. Chem. Phys. 69, 5240 (1978).
[19]B. F. Levine, C. G. Bethea, C. D. Thurmond, R. T. Lynch, and J. L. Bernstein, J. Appl. Phys. 50, 2523 (1979).
[20]D. S. Chemla, J. L. Oudar, and J. Jerphagnon, Phys. Rev. B 12, 4534 (1975).
[21]J. L. Oudar and D. S. Chemla, Opt. Commun. 13, 164 (1975).
[22]J. L. Oudar and H. LePerson, Opt. Commun. 15, 258 (1975); *ibid.* 18, 410 (1976).
[23]J. L. Oudar and D. S. Chemla, J. Chem. Phys. 66, 2664 (1977).
[24]J. L. Oudar, J. Chem. Phys. 67, 446 (1977).
[25]J. L. Oudar, D. S. Chemla, and E. Batifol, J. Chem. 67, 1626 (1977).
[26]J. L. Oudar and R. Hierle, J. Appl. Phys. 48, 2699 (1977).
[27]A. Carenco, J. Jerphagnon, and A. Perigaud, J. Chem. Phys. 66, 3806 (1977).
[28]B. F. Davydov, S. G. Kotovshchikov, and V. A. Nefedov, Sov. J. Quantum Electron. 7, 129 (1977).
[29]J. G. Bergman and G. R. Crane, J. Chem. Phys. 66, 3803 (1977).
[30]A. Dulcic and C. Sauteret, J. Chem. Phys. 69, 3453 (1978).
[31]A. Dulcic and C. Flytzanis, Opt. Commun. 25, 402 (1978).
[32]G. P. Agrawal, C. Cojan, and C. Flytzanis, Phys. Rev. B 17, 776 (1978).
[33]A. Dulcic, Chem. Phys. 37, 57 (1979).
[34]J. Tanaka, Bull. Chem. Soc. Jpn. 36, 833 (1963) and references therein.
[35]F. Bertinelli, P. Palmieri, A. Brilliante, and C. Taliani, Chem. Phys. 25, 333 (1977).
[36]B. J. Orr and J. F. Ward, Mol. Phys. 20, 513 (1971).
[37]K. D. Singer and A. F. Garito (to be published).
[38]D. A. Kleinman, Phys. Rev. 126, 1977 (1962).
[39]C. C. J. Roothaan, Rev. Mod. Phys. 23, 161 (1951).
[40]R. Pariser, J. Chem. Phys. 24, 250 (1956).
[41]D. A. Lowitz, J. Chem. Phys. 46, 4698 (1967).
[42]J. F. Ward, Rev. Mod. Phys. 37, 1 (1965).
[43]J. A. Pople and D. L. Beveridge, *Approximate Molecular Orbital Theory* (McGraw-Hill, New York, 1970).
[44]J. del Bene and H. H. Jaffe, J. Chem. Phys. 48, 1807 (1968).
[45]N. O. Lipari and C. B. Duke, J. Chem. Phys. 63, 1748 (1975).
[46]N. Mataga and K. Nishimoto, Z. Phys. Chem. (Frankfurt am Main) 13, 140 (1957).
[47]J. C. D. Brand, D. R. Williams, and T. J. Cook, J. Mol. Spectrosc. 20, 359 (1966).
[48]D. G. Lister and J. K. Tyler, Chem. Commun., 152 (1966).
[49]J. Trotter, Acta Crystallogr. 12, 884 (1959).
[50]K. N. Trueblood, E. Goldish, and J. Donohue, Acta Crystallogr. 14, 1009 (1961).
[51]T. Koopmans, Physica 1, 104 (1934).
[52]A. D. Baker, D. P. May, and D. W. Turner, J. Chem. Soc. B 22 (1968).
[53]J. W. Rabalais, J. Chem. Phys. 57, 960 (1972).
[54]O. S. Khalil, J.L. Meeks, and S. P. McGlynn, J. Am. Chem. Soc. 95, 5876 (1973).
[55]K. Kimura and S. Nagakura, Mol. Phys. 9, 117 (1965).
[56]S. Nagakura, M. Kojima, and Y. Maruyama, J. Mol. Spectrosc. 13, 174 (1964).
[57]J. F. Corbett, Spectrochim. Acta 23A, 2315 (1967).
[58]V. I. Danilova, Yu. P. Morozova, Opt. Spectrosc. (USSR) 12, 5 (1962).
[59]G. Mayer, C. R. Acad. Sci. Ser. B 267, 54 (1968).
[60]S. Keilich, IEEE J. Quantum Electron QE-5, 562 (1969).
[61]J. Jerphagnon, Phys. Rev. B 2, 1091 (1970).
[62]G. Hauchecorne, F. Kerherve, and G. Mayer, J. Phys. (Paris) 32, 47 (1971).
[63]See, for example, M. B. Ledger and P. Suppan, Spectrochim. Acta 23A, 641 (1967).
[64]A. D. Buckingham and B. J. Orr, Trans. Faraday Soc. 65, 673 (1969); Q. Rev. Chem. Soc. 21, 195 (1967).
[65]J. P. Hermann and J. Ducuing, J. Appl. Phys. 45, 5100 (1974).
[66]J. F. Ward and I. J. Bigio, Phys. Rev. A 11, 60 (1975).